Computers and Electrical Engineering 39 (2013) 1248–1259

Contents lists available at SciVerse ScienceDirect

Computers and Electrical Engineering

journal homepage: www.elsevier.com/locate/compeleceng

A novel joint parameter estimation method based on fractional ambiguity function in bistatic multiple-input multiple-output radar system ☆

Qiu Tian-Shuang [a], Li Li [a,b,*]

[a] Faculty of Electronic Information and Electrical Engineering, Dalian University of Technology, Dalian 116024, China
[b] Information Engineering College, Dalian University, Dalian 116622, China

ARTICLE INFO

Article history:
Received 11 January 2012
Received in revised form 28 February 2013
Accepted 4 March 2013
Available online 4 April 2013

ABSTRACT

Due to the three dimensional motion characteristics of the target, the received scattering signal often contains a cubic term in its phase function. The existing signal model is not appropriate to approximate parameters in this case. In this paper, we propose a new signal model to accurately estimate parameters of the target. We use a novel approach, the fractional ambiguity function, to estimate Doppler frequency parameters in the fractional Fourier transform domain. Furthermore, we also develop two sub-array models to accurately estimate the direction-of-departure and direction-of-arrival by employing the proposed fractional cross-ambiguity function based MUSIC (FCAF-MUSIC) algorithm and the fractional cross-ambiguity function based ESPRIT (FCAF-ESPRIT) algorithm. Simulation results are presented to verify the effectiveness of the proposed method.

1. Introduction

The Multiple-Input Multiple-Output (MIMO) system has attracted more and more attention for its ability to enhance system performance [1–14]. A MIMO radar system consists of transmit and receive sensors, with the transmit sensors having the ability to transmit arbitrary and independent waveforms. Among the many possible uses of a radar system, tracking and detecting targets, estimating target model parameters, and creating images of targets are some of the most common.

According to the configuration of transmit and receive antennas [1], two kinds of MIMO radars are formed, namely distributed and collocated. In the distributed MIMO radar, the antennas are widely separated in transmit array and receive array. This enables us to view the target from different angles. While the distributed radar exploits the spatial diversity, the collocated MIMO radar exploits the waveform diversity. In the collocated configuration, all the antennas are closely spaced in transmit array and receive array. A Collocated MIMO radar is also named as bistatic MIMO radar. Hence the target radar cross section (RCS) values are the same for all transmitter–receiver pairs. The RCS denotes the transformation undergone by the transmitted signal while reflecting from the surface of the target.

The multi-target parameter estimation and localization is one of the most important aspects in bistatic MIMO radar. Most existing algorithms are divided into two categories. One ignores Doppler frequency and only estimates the direction-of-departure (DOD) and the direction-of-arrival (DOA) as shown in [5–7]. The other estimates not only DOA and DOD but also time-invariant Doppler frequency as shown in [8–10]. In [8], the parallel factor is proposed to estimate DOD–DOA and Doppler frequency of bistatic MIMO radar. The received signal expression shows that it has 3-dimension array model

☆ Reviews processed and approved for publication by Editor-in-Chief Dr. Manu Malek.

* Corresponding author at: Faculty of Electronic Information and Electrical Engineering, Dalian University of Technology, Dalian 116024, China. Tel./fax: +86 411 84709573.
E-mail address: ffsimple@163.com (L. Li).

0045-7906/$ - see front matter © 2013 Elsevier Ltd. All rights reserved.
http://dx.doi.org/10.1016/j.compeleceng.2013.03.007

characteristics. Three parameters are jointly estimated from three matrices obtained from low-rank decomposition. [9] utilizes biorthogonality matrices to construct a cost function and employs an iteration algorithm to estimate the two-dimensional angles and Doppler frequency. In [10], Doppler frequency, DOA and DOD vectors are obtained by using the least square algorithm.

As mentioned above, these methods have obtained good performance in terms of parameter estimation when Doppler frequency is assumed as time-invariant. In fact, due to the three dimensional motion characteristics of the targets, the received signals may contain not only a quadratic term but also a cubic term in their phase functions. Therefore, it is not appropriate that Doppler frequency is assumed as time-invariant since it is time-variant [15–17]. In this case, the existing signal models and methods can not effectively solve this problem caused by the 3D motion of the target and provide an optimal solution. To overcome the drawbacks of the traditional models and methods, this paper constructs a novel signal model with a time varying Doppler frequency in bistatic MIMO radar system. The fractional ambiguity function is utilized to estimate Doppler frequency parameters of the new signal model, thus the time-variant Doppler frequency can be obtained.

The paper is organized as follows. Section 2 proposes a new signal array model of the bistatic MIMO radar system. In Section 3, the analysis on the fractional ambiguity function of the proposed model is presented. In Section 4, Doppler frequency parameters are estimated by searching the peak of the fractional ambiguity function (FAF) and the dechirping method, and the target is located by the proposed fractional cross-ambiguity function based MUSIC (FCAF-MUSIC) and fractional cross-ambiguity function based ESPRIT (FCAF-ESPRIT) algorithms in the fractional Fourier transform (FRFT) domain. In Section 5, we present the complexity analysis of the proposed method. In Section 6, the performance of the proposed method is studied through extensive numerical simulations. Finally, conclusions are drawn in Section 7.

2. The proposed signal model

In this section, we describe the proposed signal model for the bistatic MIMO radar system. We assume that there are Q closely spaced transmit antennas and N closely spaced receive antennas, and L targets. Fig. 1 illustrates a bistatic MIMO radar system, with half-wavelength space between adjacent elements used for both transmit array and receive array. Both transmit and receive antennas are uniform linear arrays (ULAs) and all the elements in the antennas are omni-directional. The targets appear in the far-field of transmit and receive array. The transmit antennas emit orthogonal waveforms $x_q(t)$ for $q = 1,\ldots,Q$. These signals are reflected by L targets, and are received by N receive antennas. The received signals contain cubic phase due to the three dimension motion state of these targets. If the cubic phase is ignored, the performance of parameter estimation will degrade. This paper proposes a new signal model of bistatic MIMO radar system. In general, the received signal from the nth antenna $y_n(t)$ ($n = 1,\ldots,N$) can be expressed as in (1), if the signal $x_q(t)$ is transmitted from the qth antenna and reflected by L targets.

$$y_n(t) = \sum_{l=1}^{L}\sum_{q=1}^{Q}\{\sigma_l x_q(t)\exp(j2\pi(f_l t + \mu_l t^2/2 + \kappa_l t^3/6))A_q(\varphi_l)B_n(\theta_l)\} + w_n(t), \quad 0 \leqslant t \leqslant T \tag{1}$$

where σ_l denotes the radar cross-section corresponding to the lth target. f_l, μ_l and κ_l denote the initial Doppler frequency (IDF), Doppler frequency rate (DFR) and Doppler frequency changing rate (DFCR) corresponding to the lth target, respectively. $A_q(\varphi_l) = \exp(j2\pi(q-1)d_t\sin\varphi_l/\lambda)$ is the qth element of the transmitter steering vector, where d_t is the spacing between the transmit antennas and φ_l is the DOD corresponding to the lth target. $B_n(\theta_l) = \exp(j2\pi(n-1)d_r\sin\theta_l/\lambda)$ is the nth element of the steering vector of the receiver, where d_r is the spacing between the receive antennas and θ_l is the DOA corresponding to the lth target. $w_n(t)$ is assumed to be independent, zero-mean Gaussian white noise with variance ρ^2.

Since the transmitted waves are orthogonal with each other, there are $\langle x_q, x_k\rangle = 0$, $q \neq k$ and $\|x_q\|^2 = 1$, for $k = 1,\ldots,Q$ and $q = 1,\ldots,Q$. At each receiving antenna, these orthogonal waveforms can be extracted by Q matched filters. The extracted signals by the qth matched filter can be expressed as

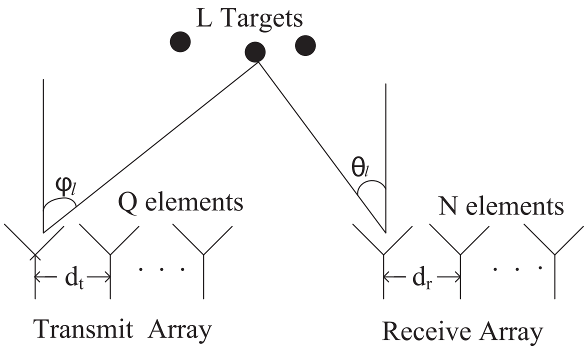

Fig. 1. Bistatic MIMO radar system.

$$y_{q,n}(t) = \sum_{l=1}^{L}\{\sigma_l \exp(j2\pi(f_l t + \mu_l t^2/2 + \kappa_l t^3/6))A_q(\varphi_l)B_n(\theta_l)\} + w_n(t), \quad 0 \leqslant t \leqslant T \tag{2}$$

3. Fractional ambiguity function analysis of the proposed signal model

The ambiguity function is a useful tool for describing the ability of a waveform to simultaneously estimate the range and range-rate (speed) of targets in active (correlation-based) radar and sonar systems [11–14]. In recent years, a new time-frequency analysis tool, the fractional Fourier transform, attracts increasing attention in signal processing society and is widely applied in detection, parameter estimation and direction of arrival estimation of the LFM signal.

With the development of the FRFT, an important relationship between the FRFT representation of the narrowband ambiguity function and its transform under the rotation operator is studied. Ref. [14] presents a new ambiguity function theory based on fractional Fourier transform and ambiguity function in order to solve the problem of the signal with cubic phase.

3.1. Fractional ambiguity function

The signal $s(t)$ with a cubic term in its phase function, also called quadratic frequency modulated signal, is defined as

$$s(t) = b_0 \exp(j2\pi(a_0 + a_1 t + a_2 t^2 + a_3 t^3)) \tag{3}$$

where b_0 is the signal amplitude, and a_i, $i = 0,1,2,3$ are signal phase factors, the amplitude and phase factors are real and unknown [14].

Instantaneous autocorrelation function $R_s(t,\tau)$ of the signal $s(t)$ is defined by

$$R_s(t,\tau) = s\left(t+\frac{\tau}{2}\right)s^*\left(t-\frac{\tau}{2}\right) \tag{4}$$

With the use of (3) and (4) can be expressed as

$$R_s(t,\tau) = b_0^2 \exp\ (j2\pi(3a_3\tau t^2 + 2a_2\tau t + a_1\tau + a_3\tau^3/4)) \tag{5}$$

For a given delay τ, $R_s(t,\tau)$ is a linear frequency modulation signal. According to the definition of FRFT in [18], the fractional ambiguity function (FAF) of the signal $s(t)$, namely the FRFT of (5), $FAF_s(\alpha,m,\tau)$ can be written as

$$FAF_s(\alpha,m,\tau) = \int_{-\infty}^{+\infty} R_s(t,\tau)K_\alpha(t,m)dt \tag{6}$$

where α is the rotation angle and m is the frequency in FRFT domain, $K_\alpha(t,m)$ is the kernel function of the fractional Fourier transform. $K_\alpha(t,m)$ can be expressed as

$$K_\alpha(t,m) = \begin{cases} \sqrt{(1-j\cot\alpha)}\exp(j\pi(t^2\cot\alpha - 2mt\csc\alpha + m^2\cot\alpha)), & \alpha \neq n\pi \\ \delta(t-m), & \alpha = 2n\pi \\ \delta(t+m), & \alpha = (2n+1)\pi \end{cases} \tag{7}$$

3.2. Fractional ambiguity function of multi-signal

Assumed that the signal $s(t)$ is a multi-component signal as $s(t) = s_1(t) + s_2(t)$, where $s_1(t)$ and $s_2(t)$ denote quadratic frequency modulated signals as (3). According to (4), instantaneous auto-correlation function $R_s(t,\tau)$ of the signal $s(t)$ can be written as

$$R_s(t,\tau) = s_1\left(t+\frac{\tau}{2}\right)s_1^*\left(t-\frac{\tau}{2}\right) + s_1\left(t+\frac{\tau}{2}\right)s_2^*\left(t-\frac{\tau}{2}\right) + s_2\left(t+\frac{\tau}{2}\right)s_1^*\left(t-\frac{\tau}{2}\right) + s_2\left(t+\frac{\tau}{2}\right)s_2^*\left(t-\frac{\tau}{2}\right) \tag{8}$$

where $s_1\left(t+\frac{\tau}{2}\right)s_1^*\left(t-\frac{\tau}{2}\right)$ and $s_2\left(t+\frac{\tau}{2}\right)s_2^*\left(t-\frac{\tau}{2}\right)$ denote instantaneous auto-correlation functions of $s_1(t)$ and $s_2(t)$, respectively. $s_1\left(t+\frac{\tau}{2}\right)s_2^*\left(t-\frac{\tau}{2}\right)$ and $s_2\left(t+\frac{\tau}{2}\right)s_1^*\left(t-\frac{\tau}{2}\right)$ denote instantaneous cross-correlation functions between $s_1(t)$ and $s_2(t)$.

According to (6) and (7), the fractional ambiguity function $FAF_s\ (\alpha,m,\tau)$ of $s(t)$ can be expressed as

$$\begin{aligned} FAF_s(\alpha,m,\tau) &= \int_{-\infty}^{+\infty} R_s(t,\tau)K_\alpha(t,m)dt \\ &= \int_{-\infty}^{+\infty} s_1\left(t+\frac{\tau}{2}\right)s_1^*\left(t-\frac{\tau}{2}\right)K_\alpha(t,m)dt + \int_{-\infty}^{+\infty} s_1\left(t+\frac{\tau}{2}\right)s_2^*\left(t-\frac{\tau}{2}\right)K_\alpha(t,m)dt \\ &+ \int_{-\infty}^{+\infty} s_2\left(t+\frac{\tau}{2}\right)s_1^*\left(t-\frac{\tau}{2}\right)K_\alpha(t,m)dt + \int_{-\infty}^{+\infty} s_2\left(t+\frac{\tau}{2}\right)s_2^*\left(t-\frac{\tau}{2}\right)K_\alpha(t,m)dt \end{aligned} \tag{9}$$

where $\int_{-\infty}^{+\infty} s_1\left(t+\frac{\tau}{2}\right)s_1^*\left(t-\frac{\tau}{2}\right)K_\alpha(t,m)dt$ and $\int_{-\infty}^{+\infty} s_2\left(t+\frac{\tau}{2}\right)s_2^*\left(t-\frac{\tau}{2}\right)K_\alpha(t,m)dt$ denote the fractional ambiguity function of $s_1(t)$ and $s_2(t)$, respectively. $\int_{-\infty}^{+\infty} s_1\left(t+\frac{\tau}{2}\right)s_2^*\left(t-\frac{\tau}{2}\right)K_\alpha(t,m)dt$ and $\int_{-\infty}^{+\infty} s_2\left(t+\frac{\tau}{2}\right)s_1^*\left(t-\frac{\tau}{2}\right)K_\alpha(t,m)dt$ denote the fractional cross-ambiguity function between $s_1(t)$ and $s_2(t)$. If these signals have different DFCR, the peak of the FAF is greater than that of the FCAF [19]. Thus, the peak of the FAF can be searched in FRFT domain. The FAF of $s(t)$ is shown in Fig. 2.

Fig. 2 shows the time-frequency plane of the FAF with $SNR = 10$ dB. We can find that the FAF is sharp-peaked.

In summary, the extracted signals $y_{q,n}(t)$ are L components signals, where L denotes the number of targets. These peaks of L fractional ambiguity functions can be obtained in FRFT domain. Thus parameters of the target can be estimated effectively.

4. Joint parameter estimation based on FCAF

In this section, the study of parameter estimation is made by taking the signal $y_{q,n,l}(t)$ as an example. The signal $y_{q,n,l}(t)$ denotes the extracted signals $y_{q,n}(t)$ corresponding to the lth target. $y_{q,n,l}(t)$ can be expressed as

$$y_{q,n,l}(t) = \sigma_l \exp(j2\pi(f_l t + \mu_l t^2/2 + \kappa_l t^3/6))\boldsymbol{A}_q(\varphi_l)\boldsymbol{B}_n(\theta_l) + w_n(t), \quad l = 1, 2, \ldots, L \tag{10}$$

4.1. Doppler frequency parameters estimation

According to (4) and (10), the instantaneous autocorrelation function $R_{y,l}(t,\tau)$ of signal $y_{q,n,l}(t)$ can be written as

$$R_{y,l}(t,\tau) = y_{q,n,l}(t+\tau/2)y^*_{q,n,l}(t-\tau/2) = \sigma_l^2 \exp\{j\pi(\kappa_l \tau t^2 + 2\mu_l \tau t + 2f_l\tau + \kappa_l\tau^3/12)\} + R_w(t,\tau) \tag{11}$$

where $R_w(t,\tau) = y_{q,n,l}(t+\tau/2)w^*(t-\tau/2) + w(t+\tau/2)y^*_{q,n,l}(t-\tau/2) + w(t+\tau/2)w^*(t-\tau/2)$ is treated as a random interference.

According to (6), the $FAF_{y,l}(\alpha,m,\tau)$ of $y_{q,n,l}(t)$ can be written as

$$\begin{aligned} FAF_{y,l}(\alpha,m,\tau) &= \int_{-\infty}^{+\infty} R_{y,l}(t,\tau)K_\alpha(t,m)dt \\ &= \sigma_l^2\sqrt{(1-j\cot\alpha)}\exp(j\pi(m^2\cot\alpha + 2f_l\tau + \kappa_l\tau^3/12))\cdot \\ &\int_{-T/2}^{+T/2} \exp(j\pi((\kappa_l\tau + \cot\alpha)t^2 + (2\mu_l\tau - 2m\csc\alpha)))dt + W(\alpha,m,\tau) \end{aligned} \tag{12}$$

where $W(\alpha,m,\tau)$ denotes FAF of noise. (12) arises the peak value when α and m meet the conditions shown in (13) and (14), as

$$\cot\alpha_l = -\kappa_l\tau \tag{13}$$

$$\mu_l\tau\sin\alpha_l = m_l \tag{14}$$

Assuming that the peak position of $FAF_{y,l}(\alpha,m,\tau)$ is (α_l, m_l), the peak value of $FAF_{y,l}(\alpha,m,\tau)$ is

$$FAF_{y,l}(\alpha_l,m_l,\tau) = \sigma_l^2\sqrt{(1-j\cot\alpha_l)}\exp\left(j\pi(m_l^2\cot\alpha_l + 2f_l\tau + \kappa_l\tau^3/12)\right)\cdot T \tag{15}$$

According to (13), DFCR κ_l is estimated by

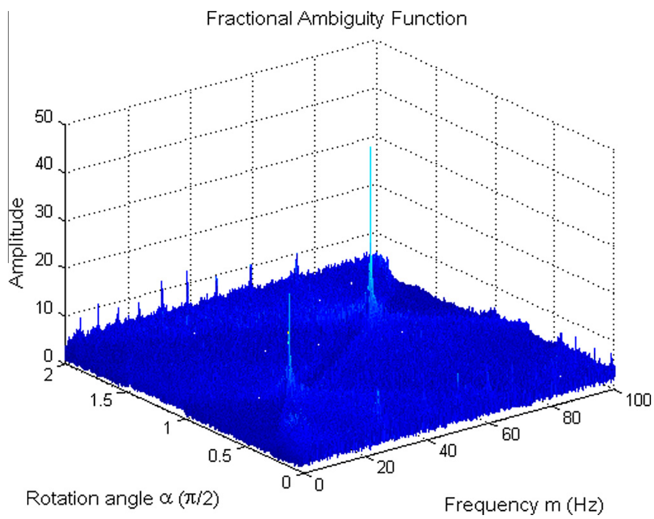

Fig. 2. Fractional ambiguity function of the signal $s(t)$.

$$\hat{\kappa}_l = -\cot\alpha_l/\tau \tag{16}$$

The dechirping method [20] is presented to estimate the initial Doppler frequency f_l and Doppler frequency rate μ_l in order to improve the estimation accuracy.

Define variable $R_1(t,\tau)$ as

$$R_1(t,\tau) = R(t,\tau)\cdot\exp(-j\pi\hat{\kappa}_l\tau t^2) \tag{17}$$

Define variable $\widetilde{R}_1(u)$ as the Fourier transform of $R_1(t,\tau)$. Assumed $\tilde{u}_l$ is the frequency corresponding to the peak of $\widetilde{R}_1(u)$, $\tilde{u}_l$ is estimated by

$$\tilde{u}_l = \arg\max_u\ \{\widetilde{R}_1(u)\} \tag{18}$$

According to (11) and (18), DFR μ_l is estimated by

$$\hat{\mu}_l = \tilde{u}_l/\tau \tag{19}$$

Define variable $y_1(t)$ as

$$y_1(t) = y_{q,n,l}(t)\cdot\exp\left(-j2\pi(\hat{\kappa}_l/6)t^3\right)\cdot\exp(-j2\pi(\hat{\mu}_l/2)t^2) \tag{20}$$

Define $\tilde{y}_1(f)$ as the Fourier transform of $y_1(t)$. So, the IDF f_l is estimated by

$$\hat{f}_l = \arg\max_f\{\tilde{y}_1(f)\} \tag{21}$$

Till now, we have achieved the proposed algorithm, the fractional ambiguity function in FRFT domain, for Doppler frequency parameters estimation in bistatic MIMO radar. We show the major steps of our algorithm as follows:

Step 1. Obtain the extracted signals $y_{q,n}(t)$.
Step 2. Compute the fractional ambiguity function of (10).
Step 3. Search the peaks of $FAF_{y,l}(\alpha,m,\tau)$ and obtain locations of these peaks (α_l, m_l).
Step 4. Estimate Doppler frequency parameters according to (16)–(21).

4.2. Joint DOA and DOD estimation

In this section, the DOD and DOA are estimated by employing the proposed FCAF-MUSIC and FCAF-ESPRIT.

According to (16), (19) and (21), we can define a variable $z_{q,n,l}(t)$ as

$$z_{q,n,l}(t) = \sigma_l\exp(j2\pi(f_lt + \mu_lt^2/2 + \kappa_lt^3/6)) + w_n(t) \tag{22}$$

The instantaneous cross-correlation function $R_{yz,l}(t,\tau)$ between $y_{q,n,l}(t)$ and $z_{q,n,l}(t)$ is defined as

$$\begin{aligned} R_{yz,l}(t,\tau) &= y_{q,n,l}(t+\tau/2)z^*_{q,n,l}(t-\tau/2) \\ &= \sigma_l^2\exp\ \{j\pi(\kappa_l\tau t^2 + 2\mu_l\tau t + 2f_l\tau + \kappa_l\tau^3/12)\}A_q(\varphi_l)B_n(\theta_l) + R_w(t,\tau) \end{aligned} \tag{23}$$

where $R_w(t,\tau) = y_{q,n,l}(t+\tau/2)w^*(t-\tau/2) + w(t+\tau/2)z^*_{q,n,l}(t-\tau/2) + w(t+\tau/2)w^*(t-\tau/2)$ is treated as a random interference.

The fractional cross-ambiguity functions $FCAF_{yz,l}(\alpha,m,\tau)$ between $y_{q,n,l}(t)$ and $z_{q,n,l}(t)$ can be expressed as

$$\begin{aligned} FCAF_{yz,l}(\alpha,m,\tau) &= \int_{-\infty}^{+\infty} R_{yz,l}(t,\tau)K_\alpha(t,m)dt \\ &= \sigma_l^2\sqrt{(1-j\cot\alpha)}A_q(\varphi_l)B_n(\theta_l)\exp(j\pi(m^2\cot\alpha + 2f_l\tau + \kappa_l\tau^3/12))\cdot \\ &\int_{-T/2}^{+T/2}\exp(j\pi((\kappa_l\tau + \cot\alpha)t^2 + (2\mu_l\tau - 2m\csc\alpha)))dt + W(\alpha,m,\tau) \end{aligned} \tag{24}$$

where $W(\alpha,m,\tau)$ denotes the fractional ambiguity function of the noise. $FCAF_{yz,l}(\alpha,m,\tau)$ arises the peak value when α and m meet the conditions shown in (13) and (14), and the position of the peak is also located at (α_l, m_l). The peak value of $FCAF_{yz,l}(\alpha,m,\tau)$ is

$$FCAF_{yz,l}(\alpha_l,m_l,\tau) = \sigma_l^2\sqrt{(1-j\cot\alpha_l)}A_q(\varphi_l)B_n(\theta_l)\exp\left(j\pi\left(m_l^2\cot\alpha_l + 2f_l\tau + \kappa_l\tau^3/12\right)\right)\cdot T \tag{25}$$

With the use of (15) and (25) can be expressed as

$$FCAF_{yz,l}(\alpha_l,m_l,\tau) = A_q(\varphi_l)B_n(\theta_l)FAF_{y,l}(\alpha_l,m_l,\tau) \tag{26}$$

At (α_l, m_l), the fractional cross-ambiguity function $MCAF_{yz,l}(\alpha_l,m_l,\tau)$ between (2) and (22) can be expressed as

$$MCAF_{yz,l}(\alpha_l, m_l, \tau) = FCAF_{yz,l}(\alpha_l, m_l, \tau) + \sum_{\rho \neq l}^{L} FCAF_{yz,l\rho}(\alpha_l, m_l, \tau) \tag{27}$$

Because the amplitudes of FCAF of different targets are very low at (α_l, m_l) in FRFT domain, these signals are not considered as random interfering. Therefore, (27) can be rewritten as

$$MCAF_{yz,l}(\alpha_l, m_l, \tau) = A_q(\varphi_l)B_n(\theta_l)FAF_{y,l}(\alpha_l, m_l, \tau) \tag{28}$$

Selecting L peak points $MCAF_{yz,l}(\alpha_l, m_l, \tau)$ for $l = 1, \ldots, L$ as observed data at the receiver, the output of the nth receive antenna in the FRFT domain can be expressed as

$$\boldsymbol{MCAF}_{yz}^{(n)} = \left[MCAF_{yz,1}^{(n)}(\alpha_1, m_1, \tau) \quad MCAF_{yz,2}^{(n)}(\alpha_2, m_2, \tau) \quad \ldots \quad MCAF_{yz,L}^{(n)}(\alpha_L, m_L, \tau) \right] \tag{29}$$

The vector of the receiver outputs can be modeled as

$$\boldsymbol{R} = \boldsymbol{GAB} + \boldsymbol{N} \tag{30}$$

where $\boldsymbol{R}$ is

$$\boldsymbol{R} = \left[\boldsymbol{MCAF}_{yz}^{(1)} \quad \boldsymbol{MCAF}_{yz}^{(2)} \quad \ldots \quad \boldsymbol{MCAF}_{yz}^{(N)} \right]^T \tag{31}$$

$\boldsymbol{G}$ is

$$\boldsymbol{G} = diag\{ FAF_{y,1}(\alpha_1, m_1, \tau) \quad FAF_{y,2}(\alpha_2, m_2, \tau) \quad \ldots \quad FAF_{y,L}(\alpha_L, m_L, \tau) \} \tag{32}$$

$\boldsymbol{A}$ is

$$\boldsymbol{A} = diag\{ A_q(\varphi_1) \quad A_q(\varphi_2) \quad \ldots \quad A_q(\varphi_L) \} \tag{33}$$

and $\boldsymbol{B}$ is

$$\boldsymbol{B} = [\boldsymbol{B}_1 \quad \boldsymbol{B}_2 \quad \ldots \quad \boldsymbol{B}_L] \tag{34}$$

where $\boldsymbol{B}_l$ is

$$\boldsymbol{B}_l = [B_1(\theta_l) \quad B_2(\theta_l) \quad \ldots \quad B_N(\theta_l)]^T \tag{35}$$

where $(\cdot)^T$ and diag$(\cdot)$ denote the transpose and the diagonal matrix respectively.

Both receive sub-arrays $\boldsymbol{R}_1$ and $\boldsymbol{R}_2$ constructed in this paper can be expressed by

$$\boldsymbol{R}_1 = [\boldsymbol{R}_{1,1} \quad \boldsymbol{R}_{1,2} \quad \ldots \quad \boldsymbol{R}_{1,N}]^T = \boldsymbol{BG} + \boldsymbol{N}_1 \tag{36}$$

$$\boldsymbol{R}_2 = [\boldsymbol{R}_{q,1} \quad \boldsymbol{R}_{q,2} \quad \ldots \quad \boldsymbol{R}_{q,N}]^T = \boldsymbol{BAG} + \boldsymbol{N}_2, \quad q \neq 1 \tag{37}$$

According to (36) and (37), FCAF-MUSIC and FCAF-ESPRIT algorithms are proposed to estimate DOAs and DODs, respectively.

The correlation matrix $\boldsymbol{R}_{R_1R_1}$ of the subarray $\boldsymbol{R}_1$ is defined as

$$\boldsymbol{R}_{R_1R_1} = E\left[\boldsymbol{R}_1\boldsymbol{R}_1^H\right] = \boldsymbol{B}E[\boldsymbol{GG}^H]\boldsymbol{B}^H + E[\boldsymbol{N}^H] + \boldsymbol{B}E[\boldsymbol{GN}^H] + E[\boldsymbol{NG}^H]\boldsymbol{B}^H \tag{38}$$

where $(\cdot)^H$ denotes the Hermitian transpose, and $E[\cdot]$ denotes the statistical expectation.

As the signal $\boldsymbol{G}$ is independent of the noise $\boldsymbol{N}$, (38) can be rewritten as

$$\boldsymbol{R}_{R_1R_1} = \boldsymbol{B}E[\boldsymbol{GG}^H]\boldsymbol{B}^H + \sigma^2\boldsymbol{I} = \boldsymbol{BR}_{GG}\boldsymbol{B}^H + \sigma^2\boldsymbol{I} \tag{39}$$

where matrix $\boldsymbol{R}_{GG}$ is the signal covariance matrix and $\boldsymbol{I}$ is the unit matrix.

Taking eigen value decomposition to matrix $\boldsymbol{R}_{GG}$, we can get

$$\boldsymbol{R}_{R_1R_1} = \boldsymbol{U}_G\sum_G\boldsymbol{U}_G^H + \boldsymbol{U}_N\sum_N\boldsymbol{U}_N^H \tag{40}$$

where the column vectors of $\boldsymbol{U}_G$ and $\boldsymbol{U}_N$ are the eigenvectors spanning the signal subspace and noise subspace of $R_{R_1R_1}$ respectively, with the associated eigenvalues on the diagonals of $\sum_G$ and $\sum_N$.

Spatial spectrum of FAF-MUSIC in fractional Fourier domain can be obtained based on classical MUSIC algorithm, which can be expressed as

$$P(\theta) = \frac{1}{\boldsymbol{B}^H(\theta)\boldsymbol{U}_N\boldsymbol{U}_N^H\boldsymbol{B}(\theta)} \tag{41}$$

Searching spectral peak of $P(\theta)$, we can get the DOA estimator θ_l.

We define

$$\mathbf{C}_{11} = \mathbf{R}_{R_1R_1} - \sigma^2\mathbf{I} = \mathbf{B}\mathbf{R}_{GG}\mathbf{B}^H \tag{42}$$

and

$$\mathbf{C}_{12} = \mathbf{R}_{R_1R_2} - \sigma^2\mathbf{Z} = \mathbf{B}\mathbf{A}\mathbf{R}_{GG}\mathbf{B}^H \tag{43}$$

where $\mathbf{Z}$ is showed as $\mathbf{Z} = \begin{bmatrix} 0 & & & 0 \\ 1 & 0 & & \\ & 1 & \ldots & \\ 0 & & 1 & 0 \end{bmatrix}$.

According to (34) and (35), we can get

$$\mathbf{C}_{12}\mathbf{C}_{11}^{\#}\mathbf{B} = \mathbf{B}\mathbf{A} \tag{44}$$

where $()^{\#}$ denotes the Moore–Penrose pseudo-inverse.

According to (33), the matrix $\mathbf{A}$ can be written as

$$\mathbf{A} = \mathbf{B}^{\#}\mathbf{C}_{12}\mathbf{C}_{11}^{\#}\mathbf{B} \tag{45}$$

Therefore, the DOD estimator φ_l is estimated by

$$\varphi_l = \arcsin(\arg(g_l)/(q-1)\pi) \tag{46}$$

where g_l is the element of the principal diagonal of matrix $\mathbf{A}$, $\arg(g_l)$ stands for the phase of g_l.

From the above equations, the DOA and DOD estimators of target can be estimated in the identical iterative process, so the angles can be paired automatically.

Till now, we have achieved the proposal for FCAF-MUSIC and FCAF-ESPRIT algorithms for DOD and DOA estimation in bistatic MIMO radar. We show the major steps of our algorithm as follows:

Step 1. Construct two matrixes $\mathbf{R}_1$ and $\mathbf{R}_2$ based on these peaks of fractional cross-ambiguity function;
Step 2. Perform eigen-decomposition operation for the covariance matrix $\mathbf{R}_{R_1R_1}$ to obtain $\mathbf{U}_N$;
Step 3. Find the K largest peaks of $P(\theta)$ with respect to (41) to get the estimate of DOAs by searching θ.
Step 4. Get the estimated transmit steering vector according to (42) and (43), and get the estimate of DODs with (46).

In bistatic radars the target location may be specified either with respect to the receiver or the transmitter. Given the DOD and DOA, the calculation of the target range is then straightforward [17]. For simplicity, we assume that the transmitter and the receiver are both stationary and focus on the target motion alone. Through multiple times computing, we can obtain target velocity and range in each moment. Thus the motion state of target is estimated.

5. Complexity analysis

In this section we assess the computation load of the proposed method.

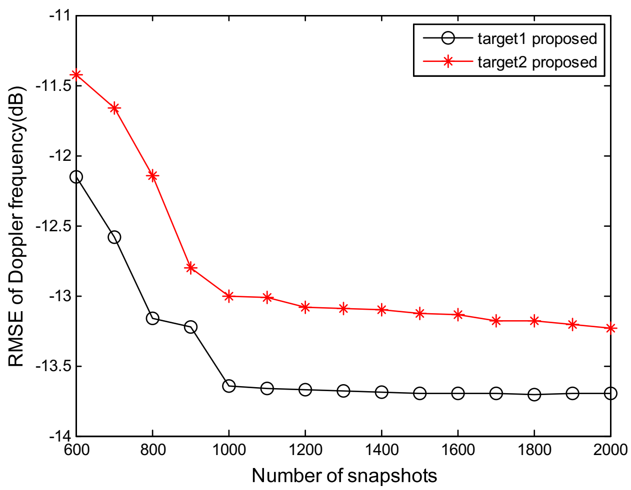

Fig. 3. RMSE of Doppler estimates versus number of snapshots M.

5.1. Doppler frequency parameters

Three Doppler frequency parameters are estimated by searching the peak of the fractional ambiguity function which is the FRFT of the instantaneous autocorrelation function. This involves M complex multiplications for obtaining $y_{q,n,l}(t+\tau/2)y^*_{q,n,l}(t-\tau/2)$ and $M\log_2 M$ multiplications for computing the FRFT. Furthermore, one time and twice FFT are computed to estimate the DFR and IDF, respectively. Thus, the total number of complex multiplication to estimate Doppler frequency parameters is $O(M+3M\log_2 M)\approx O(3M\log_2 M)$.

5.2. DOD and DOA

The L peak points $MCAF_{yz,l}(\alpha_l, m_l, \tau)$ for $l=1,\ldots,L$ are selected as observed data to estimate DOA and DOD. The complexity of FCAF-MUSIC algorithm is $O(N^3+JNP)$, where J is the total number of spectral points [21]. The proposed FCAF-ESPRIT algorithm requires $O(N^3+JNP+Q^3)$.

In the following section, we present the simulation results in order to demonstrate the performance of the proposed algorithm.

6. Simulation results

The considered bistatic MIMO radar is composed of $Q=4$ transmit antennas and $N=6$ receive antennas. The number of target is $L=2$ located at the positions $(\varphi_1,\theta_1)=(50°, 30°)$ and $(\varphi_2,\theta_2)=(20°, 60°)$. Doppler frequency parameters are $f_1=8$,

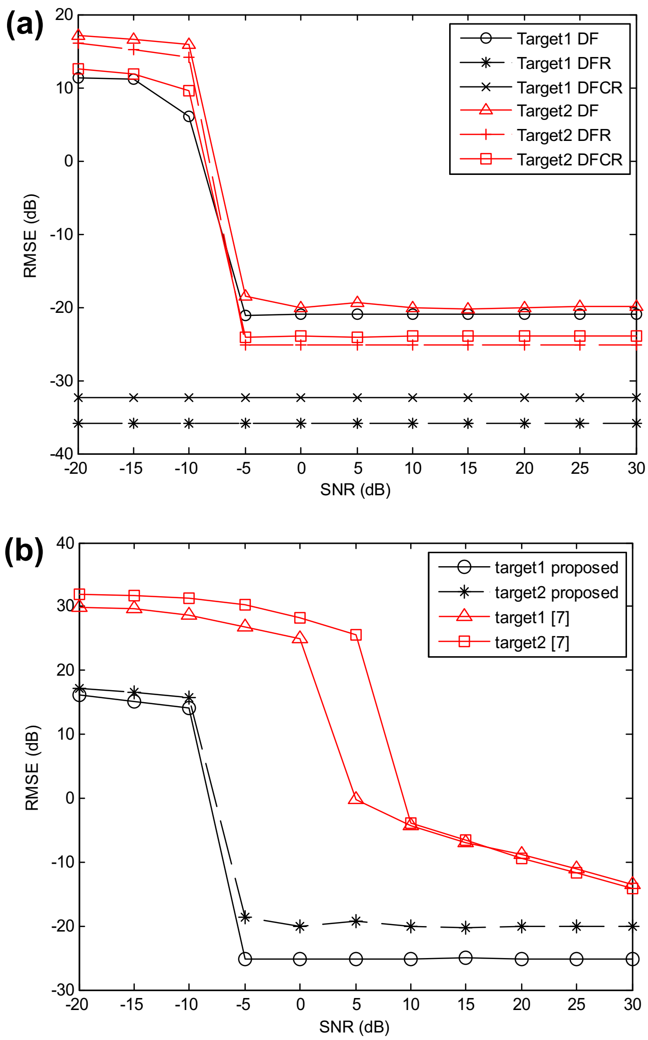

Fig. 4. RMSE of Doppler parameters estimation (a) and Doppler estimation (b) versus SNR.

$\mu_1 = 0.5$, $\kappa_1 = 0.3$, $f_2 = 12$, $\mu_2 = 0.9$ and $\kappa_2 = -0.6$, respectively. The number of Monte Carlo iterations is 300 in all simulations. We use the root-mean-square error (RMSE) [8] of the lth target $RMSE_{\xi_l} = \sqrt{\frac{1}{K}\sum_{k=1}^{k=K}(\hat{\xi}_{lk} - \xi_l)^2}$ as the performance measurement, where K is the Monte-Carlo trial number, $\hat{\xi}_{lk}$ is the estimate of the kth experiment and ξ_l is its truth value.

In the following simulation experiments, we study the resolution capability and estimation accuracy of the proposed method and the method in [7] as a function of the signal to noise ratio (SNR). We consider the influence of the number of snapshots, the array element spacing and SNR to the performance of the proposed method.

Simulation 1: Number of snapshots N_s

Fig. 3 plots the RMSE of the Doppler frequency estimates versus the number of snapshots. In this simulation, the signal to noise ratio is set as $SNR = 10$ dB. Fig. 3 indicates that the RMSE tends to be stable when the number of snapshots $N_s \geqslant 1000$. We adapt $N_s = 1000$ in the later simulations. From Fig. 3 we also find that the RMSE of Doppler increases versus the increase of Doppler.

Simulation 2: Signal to noise ratio

Fig. 4a and b depicts the RMSE as a function of SNR when $N_s = 1000$. Fig. 4a shows the RMSE of Doppler frequency parameters estimation of the proposed method versus SNR. Fig. 4b shows the RMSE of Doppler estimation of the proposed method and the method in [7].

From Fig. 4a, we see when SNR is higher than -5 dB, the RMSE curves tend to be stable. When SNR is below -5 dB, the FAF of the signal are merged by noises and its peak can not be detected easily. The performance of parameter estimation would

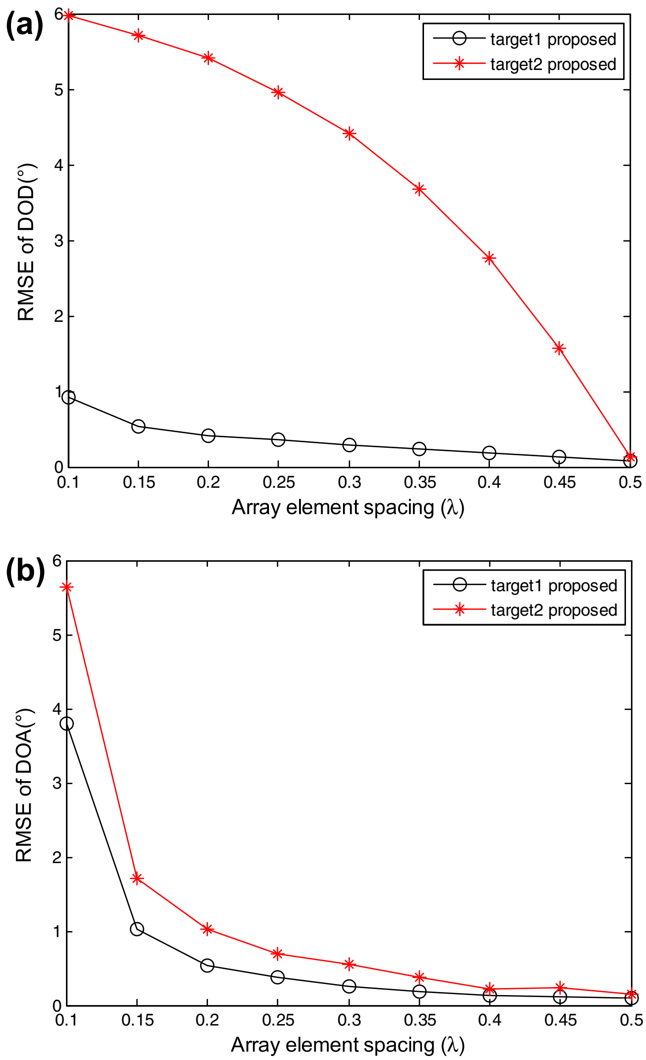

Fig. 5. RMSEs of the DOD (a) and DOA (b) estimation versus the array element spacing.

deteriorate in this case. From Fig. 4b, the performance of the proposed method is significantly better than that of the method in [7].

For a given delay τ, the instantaneous autocorrelation function of the Quadratic frequency modulated signal is an expression of linear frequency modulation signal, and the FRFT of the linear frequency modulation signal has the energy-concentrated characteristics, while noise does not have such characteristics. Therefore Doppler frequency parameters can be estimated by searching the peak of the fractional ambiguity function. The received signal has a low SNR in bistatic MIMO radar system, so the proposed method is more suitable for this application. It is important to find better peak searching method so as to improve the estimation accuracy.

Simulation 3: Array element spacing

Fig. 5a and b shows the RMSE of the DOD and DOA for various values of the array element spacing of antennas. In this simulation, the number of snapshots N_s is 1000, and the signal to noise ratio is set as $SNR = 10$ dB. The array element spacing is $d \leqslant \lambda/2$ to enable unambiguous estimation of the angle [22,23].

From Fig. 5, we can find that the estimation of the DOD and DOA gives better performance when the array element spacing is set as 0.5λ. We adapt $d_t = d_r = 0.5\lambda$ in the later simulations. From Fig. 5, we also obtain that the RMSEs of the DOD and DOA increase versus the increase of the angle, and such effect is particularly significant for the DOD estimation.

Simulation 4: Signal to noise ratio

Fig. 6a and b shows RMSE curves for DODs and DOAs estimation of the proposed method, the method in [7], FCAF-MUSIC and FCAF-ESPRIT versus SNR. In this simulation, $M = 1000$ and $d_t = d_r = 0.5\lambda$ are set. FCAF-MUSIC and FCAF-ESPRIT algorithms are run with truth values of the Doppler frequency parameters. The proposed method is run in the condition of the estimated Doppler frequency parameters. As we can see, the proposed method, FCAF-MUSIC and FCAF-ESPRIT give better performance

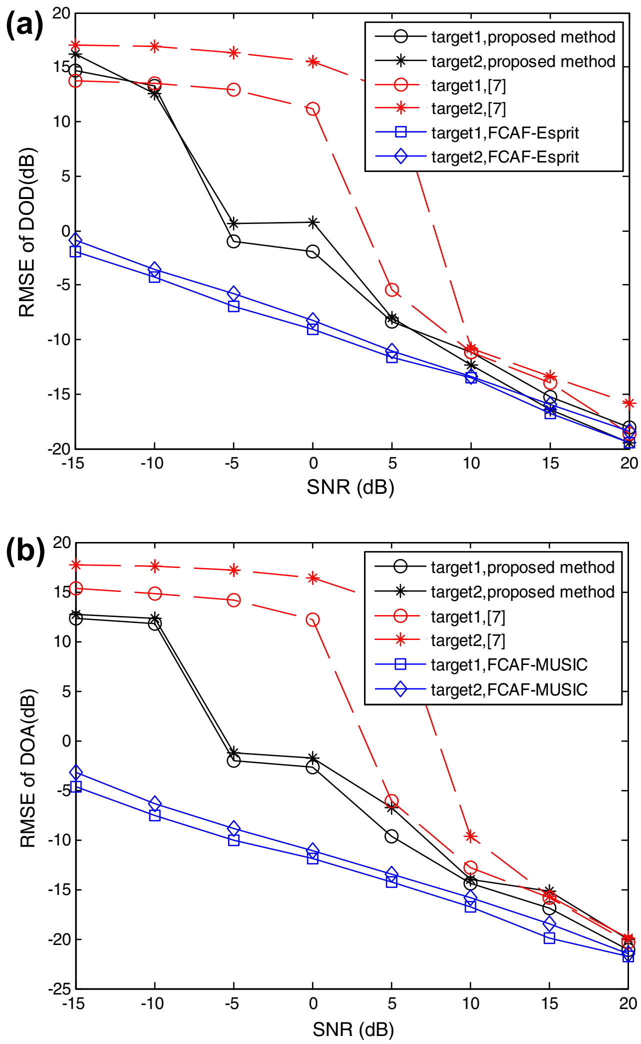

Fig. 6. RMSE of the DODs (a) and DOAs (b) estimation versus SNR.

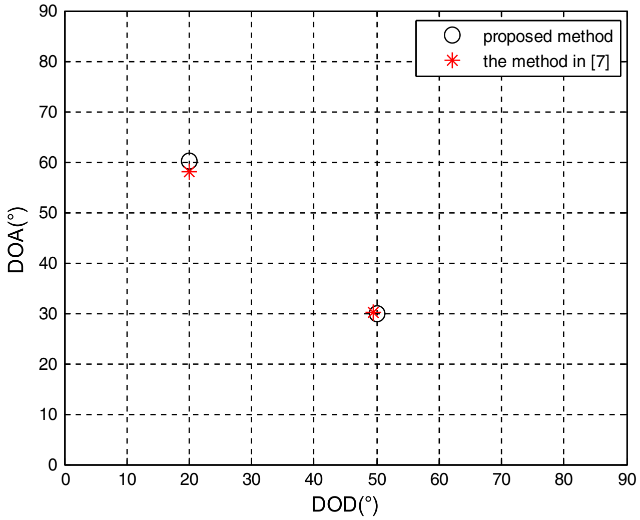

Fig. 7. Location estimation result of two targets.

than the method in [7] in the condition of low SNR. From these figures, we also find that the estimation performance of the Doppler frequency parameters affects the estimation performances of the DOD and DOA.

Simulation 5: The estimated result of DOAs and DODs

Fig. 7 illustrates the scatter grams of the DOAs and DODs estimated by the proposed method and the method in [7] based on 100 independent trials under the hypothesis that SNR is equal to 7 dB and other simulation conditions are exactly the same as those described in Simulation 4. From Fig. 7, we can observe that the proposed method provides a more precise location estimate than the method in [7].

7. Conclusion

In this paper, the fractional ambiguity function in FRFT domain is applied to the joint estimation of Doppler frequency parameters, the DODs and DOAs in bistatic MIMO radar system. Since the target has three dimensional motion states, the received signals reflected from these targets often contain cubic phase. This paper proposes a new signal model since the existing ones are not appropriate to approximate the parameters in this case. For a given delay, the instantaneous autocorrelation function of the signal with cubic phase is an expression of linear frequency modulation signal. Hence, this paper proposes a new approach to estimate these parameters in FRFT domain. We estimate Doppler frequency parameters by searching peak of the fractional ambiguity function. We also develop two sub-array models to accurately estimate the DOD and the DOA by employing the FCAF-MUSIC algorithm and the FACF-ESPRIT algorithm. In Simulation results section, we discuss the effects of various parameters in terms of the RMSE, including the number of snapshots, the array element spacing, and the SNR. We also compare the performance of the proposed method with that of the others. Simulation results are presented to verify the effectiveness of the proposed method.

Acknowledgments

The authors are grateful to three anonymous reviewers for their constructive comments and suggestions, which helped improve the manuscript. This work was partly supported by the National Science Foundation of China under Grants 61172108 and 61139001.

References

[1] Gogineni S, Nehorai A. Target estimation using sparse modeling for distributed MIMO radar. IEEE Trans Signal Process 2011;59(11):5315–25.
[2] Stoica P, Li J, Xie Y. On probing signal design for MIMO radar. IEEE Trans Signal Process 2007;55(8):4151–61.
[3] Nagaradjane P, Krishnan L, Vasan ASS. Performance analysis of multicell MIMO MC DS/CDMA system with MMSE user-ordered SIC technique. Comput Electr Eng 2012;38:105–15.
[4] Kumaratharan N, Danajayan P. Performance improvement in detection and estimation of MC-CDMA systems over MIMO channels. Comput Electr Eng 2010;36:224–33.
[5] Chen CY, Vaidyanathan PP. MIMO radar space–time adaptive processing using prolate spheroidal wave functions. IEEE Trans Signal Process 2008;56(2):623–35.
[6] Li CC, Liao GS, Zhu SQ, Wu SY. An ESPRIT-like algorithm for coherent DOA estimation based on data matrix decomposition in MIMO radar. Signal Process 2011;91(8):1803–11.

[7] Bencheikh ML, Wang YD, He HY. Polynomial root finding technique for joint DOA DOD estimation in bistatic MIMO radar. Signal Process 2010;90:2723–30.
[8] Zhang JY, Zheng ZD, Li XB. An algorithm for DOD–DOA and Doppler frequency joint estimating of bistatic MIMO radar. J Electron Inform Technol 2010;32(8):1843–8.
[9] Lu H, Feng DZ, He J, Xiang C. A novel method for target localization and doppler frequency estimation in bistatic MIMO radar. J Electron Inform Technol 2010;32(9):2167–71.
[10] Zhang XF, Xu LY, Xu L, Xu DZ. Direction of departure (DOD) and direction of arrival (DOA) estimation in MIMO radar with reduced-dimension MUSIC. IEEE Commun Lett 2010;14(12):1161–3.
[11] Li J, Stoica P. MIMO radar with colocated antennas. IEEE Signal Process Mag 2007:106–14.
[12] Borden B. On the fractional wideband and narrowband ambiguity function in radar and sonar. IEEE Signal Process Lett 2006;13(9):545–8.
[13] Geoffrey SA, Daniel RF, Frank CR. MIMO radar ambiguity functions. IEEE J Select Top Process 2007;1(1):167–77.
[14] Chen Z, Wang HY, Qiu TS. The study of ambiguity function based on fractional fourier transform. Signal Process 2003;19(6):499–502 (In Chinese).
[15] Vilaipornsawai U, Leib H. Joint data detection and channel estimation for fading unknown time-varying doppler environment. IEEE Trans Commun 2010;58(8):2277–91.
[16] Vincent F, Besson O. Estimating time-varying DOA and Doppler shift in radar array processing. IEE Proc Radar Sonar Navigation 2000;147(6):285–90.
[17] Tsao T, Slamani M, Varshney P, Weiner D, Schwarzlander H. Ambiguity function for a bistatic radar. IEEE Trans Aerospace Electron Syst 1997;33(3):1041–51.
[18] Tao R, Deng B, Wang Y. Fractional Fourier transform and its applications. Beijing: Tsinghua University; 2009. p. 285–96.
[19] Qu Q, Jin ML, Kim JM. FRFT based parameter estimation of the quadratic FM signal. Chin J Electron 2010;19(3): 463–7.
[20] de Witt JJ, Nel WAJ. Range doppler dynamic considerations for dechirp on receive radar. In: Proceedings of the 5th European radar conference; October 2008. p. 136–9.
[21] Rubsamen M, Gershman AB. Direction-of-arrival estimation for nonuniform sensor arrays: from manifold separation to fourier domain MUSIC methods. IEEE Trans Signal Process 2009;57(2):588–99.
[22] Fishler E, Haimovich A, Blum R, Chizhik D, Cimini L, Valenzuela R. MIMO radar: an idea whose time has come. In: Proc IEEE radar conf; 2004. p. 71–8.
[23] Li J, Stocia P. MIMO radar with collocated antennas. IEEE Signal Process Mag 2007:106–14.

Tianshuang Qiu received the B.S. degree from Tianjin University in 1983, the M.S. degree from Dalian University of Technology in 1993, and the Ph.D. degree from Southeastern University in 1996. He is currently a professor in the Department of Electronic Engineering, Dalian University of Technology. His research interests include Non-Gaussian signal processing, adaptive signal processing, and biomedical signal processing.

Li Li received the B.S. and M.S. degrees from Liaoning normal university of China in 2002 and 2005, respectively. She is now a Ph.D. student for signal and information processing in Dalian University of Technology. Her research interests include array signal processing and estimating parameter estimation in MIMO radar systems.